3.6.8 High-performance liquid chromatography (HPLC) analytics

Due to their aromaticity, methanolic extracts of flavonoids exhibit two major absorption peaks in the UV/VIS region of the light spectrum in the range of (240 to 400) nm [130]. However, even the more simple phenyl propanoids (e.g. cinnamic acids) show absorption of light in the UV/VIS-region.
Methanolic extracts of flavonoids and phenyl propanoids were analyzed by HPLC using a photo diode array (PDA)-detector, which was set to record in the range of (200 to 400) nm. HPLC runs were performed on a reverse-phase C-18 end-capped column (YMC-Pack ODS-A; YMC Europe, Dinslaken, Germany) with a pore size of 120 Å. The mobile phase was aqueous acetonitrile supplemented with 0.2 % formic acid. The flow was kept constant at 0.8 ml/min. 10 µl *O*-MT enzyme assay extract (3.6.3) were injected and analyzed using an acetonitrile gradient starting with 5 % acetonitrile (4 min). The acetonitrile content was increased to 100 % in 21 min and was kept at 100 % for 5 min. Peaks were integrated from the 280 nm trace using the software provided by the manufacturer of the device.

3.6.9 Liquid chromatography-tandem mass spectrometry (LC-MS/MS) measurements

The positive and negative ion high resolution electrospray ionization (ESI) and collsion induced dissociation (CID) MSn spectra as well as higher-energy collisional dissociation (HCD) MS/MS spectra were obtained from an Orbitrap Elite mass spectrometer (Thermo Fisher Scientific, Bremen, Germany) equipped with an heated-electrospray ionization (H-ESI) ion source (positive spray voltage 4.5 kV, negative spray voltage 3.5 kV, capillary temperature 275 °C, source heater temperature 250 °C, fourier transform mass spectrometry (FTMS) resolving power (RP) 30 000). Nitrogen was used as sheath and auxiliary gas. The MS system was coupled with an ultra-high performance liquid chromatography (UHPLC) system (Dionex UltiMate 3000, Thermo Fisher Scientific), equipped with a RP-C18 column (particle size 1.9 µm, pore size 175 Å, 50 x 2.1 mm inner diameter, Hypersil GOLD, Thermo

Fisher Scientific, column temperature 30 °C) and a photodiode array detector ((190 to 400) nm, Thermofisher Scientific). For the UHPLC a gradient system was used starting from H_2O:CH_3CN 95:5 (each containing 0.2 % formic acid) raised to 0:100 within 10 min and held at 0:100 for further 3 min. The flow rate was 150 µl/min.

The mass spectra (buffer gas: helium) were recorded using normalized collision energies (NCE) of (30 to 45) % and (75 to 100) % for CID and HCD mass spectra respectively (see Appendix). The instrument was externally calibrated using the Pierce® LTQ Velos ESI positive ion calibration solution (product number 88323, Thermofisher Scientific, Rockford, IL, 61105 USA) and the Pierce® LTQ Velos ESI negative ion calibration solution (product number 88324, Thermofisher Scientific, Rockford, IL, 61105 USA) for positive and negative ionization mode respectively.

Comparative CID and HCD MS/MS studies for the characterization of flavanoid aglycones

Benjamin Weigel[1,a], **Annegret Laub**[1,b], **Jürgen Schmidt**[1,c], **Ludger A. Wessjohann**[1,d]

Contact: bweigel@ipb-halle.de[a], alaub@ipb-halle.de[b], law@ipb-halle.de[d]

Affiliation: Leibniz-Institute of Plant Biochemistry, Department of Bioorganic Chemistry[1]

Keywords: tandem mass spectrometry, LCMS, flavonoids

Abstract

Flavonoids are an important class of natural compounds and make up a large part of the world's biomass. Due to their anti-inflammatory and anti-oxidant properties, many health benefits are associated with flavonoids and there is a growing interest to use flavonoids in medicinal and dietary contexts. The availabilty of methods that provide for a quick and reliable identification of flavonoids from different sources is therefore essential. In this work a range of flavonoids was studied using liquid chromatography coupled mass-spectrometry (LC/MS). Two modes of activation, namely CID and HCD, were evaluated to study fragmentation of flavonoids from their $[M+H]^+$ molecular ions. It was found, that HCD outperformed CID in the ring-fragmentations of methylated flavonoids. Together, both methods provide complementary information that can be used to distinguish different types of flavonoids.

5.1 Introduction

Liquid chromatography-tandem mass spectrometry (LC-MS/MS) has been widely used for the on-line identification of compounds from complex samples, such as crude mixtures from plant or bacterial extracts and is an unexpendable method in the field of metabolomics [56, 123, 127, 165].

Ionization of samples in LC-MS/MS instruments is usually achieved by mild methods operating at atmospheric pressure, such as electrospray ionization (ESI) [208] or atmospheric pressure chemical ionisation (APCI) [79]. However, small molecules rarely produce fragment ions under these conditions and usually only the *m/z* o f the molecular ion is observed. A range of different approaches has been used to circumvent this draw-back. The most direct approach is to use electron impact (EI), where the analytes are bombarded with electrons, for ionization. However, EI is a vacuum method and the coupling with liquid chromatography (LC)-systems is not trivial [199]. In order to still generate fragments in liquid chromatography coupled mass-spectrometry (LC/MS) MS/MS methods such as collsion induced dissociation (CID) or surface-induced dissociation (SID) were developed [182].

Flavonoids comprise a huge chemical space, with millions of theoretical structures [209]. Due to their biological activities and associated health benefits, applications to quickly identify and characterize these compounds are of special interest. Already, a number of studies have been published that show how MS/MS-approaches using CID can aid in the structural characterization of flavonoids [28, 40, 58, 67, 83, 116, 120, 129, 134, 135]. Researchers have reported that specifc patterns of fragmentation along the C-ring can be observed for different classes of flavonoids and can help differentiate between them [40, 129]. However, it was found that the cleavage of the C-ring is less commonly observed for flavonoids methylated at the B-ring, while the loss of small molecules becomes predominant [40, 129].

Fragments of flavonoid aglycones can be represented by a systematic nomenclature first proposed by Ma *et al.* [129]. The labels ${}^{i,j}\mathrm{A}^{+}$ and ${}^{i,j}\mathrm{B}^{+}$ refer to fragments containing an intact A or B ring, with the superscripts *i* and *j* denoting the bonds of the C-ring that were broken (Figure 5.1). In this work the complementarity of two activation methods, CID and higher-energy collisional dissociation (HCD), for the structural characterization of flavonoids (Table 5.1), especially those methylated at the B-ring, in positive ionization mode was evaluated.

Table 5.1.: *Substrates studied in this work. Three classes of flavonoids were tested: flavanones (**1-5**), flavones (**6-10**) and flavonols (**11-15**). The topology of the bond in the C-ring specifying flavanones or flavones/flavonols is denoted with **s** (single) or **d** (double), respectively.*

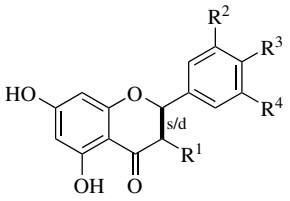

	name	$[M+H]^+$	s/d	R^1	R^2	R^3	R^4
1	naringenin	273	s	H	H	OH	H
2	eriodictyol	289	s	H	OH	OH	H
3	ponciretin	287	s	H	H	OCH_3	H
4	hesperetin	303	s	H	OH	OCH_3	H
5	homoeriodictyol	303	s	H	OCH_3	OH	H
6	apigenin	271	d	H	H	OH	H
7	luteolin	287	d	H	OH	OH	H
8	acacetin	285	d	H	H	OCH_3	H
9	diosmetin	301	d	H	OH	OCH_3	H
10	chrysoeriol	301	d	H	OCH_3	OH	H
11	kaempferol	287	d	OH	H	OH	H
12	quercetin	303	d	OH	OH	OH	H
13	myricetin	317	d	OH	OH	OH	OH
14	kaempferide	301	d	OH	H	OCH_3	H
15	isorhamnetin	317	d	OH	OCH_3	OH	H

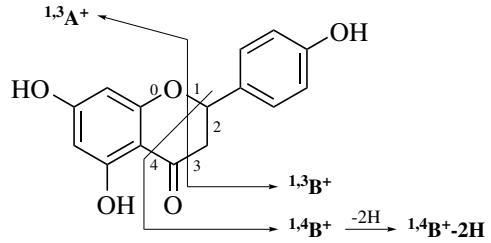

Figure 5.1.: Ion fragment nomenclature of flavonoid aglycones as proposed by Ma et al., illustrated on naringenin. Ions are labelled according to the ring they contain and the positions of the C ring that were broken. Thus $^{1,3}A^+$, contains the ring A and bonds 1 and 3 of the C ring were broken.

5.2 Fragmentation of flavanones

Positive ionization MS^2 spectra of flavanones (Table B.11) are mostly characterized by a base peak at *m/z* 153, which corresponds to the A-ring of the flavonoid skeleton (Figure 5.2). Even when *m/z* 153 was not the base peak, it was still dominant in the spectrum with intensities ranging between 20 % and 77 %. Peaks corresponding to the molecular ions $[M+H]^+$ were not observed for any of the flavanones. The structure of the ion $^{1,3}A^+$ corresponding to *m/z* 153 is the same for all compounds (**1**) to (**5**) (Figure 5.2). Peaks corresponding to mass-to-charge ratio (*m/z*) values of the respective ($^{1,4}B^+$-2H) ions are also present in the mass spectra of each flavanone. Apart from the ions $^{1,3}A^+$ and ($^{1,4}B^+$-2H), the CID- and HCD-mass spectra of the flavanones differ significantly. CID mainly triggers neutral losses directly from the molecular ion. Losses of water (18 Da) and one or two ketene units (C_2H_2O, 42 Da) are predominant and afford ions of relatively high masses (Figure 5.2) [95].

Fragment ions from cleavage of the C-ring ($^{1,3}A^+$ and ($^{1,4}B^+$-2H)) further decomposed under the higher energy conditions in HCD experiments. Thus, the resulting HCD spectra generally display smaller *m/z* than the CID spectrum (Figure 5.4). Increasing the normalized collision energy (NCE) from 75 to 100 % in HCD experiments further increased fragmentation. This is made clear by the increasing intensities of smaller fragments upon raising the NCE (Figure 5.4).

Further fragmentation of ion ($^{1,4}B^+$-2H) seems to depend on the substituents of the B-ring. Only ($^{1,4}B^+$-2H) from eriodictyol (**2**) loses a water, as suggested by a peak

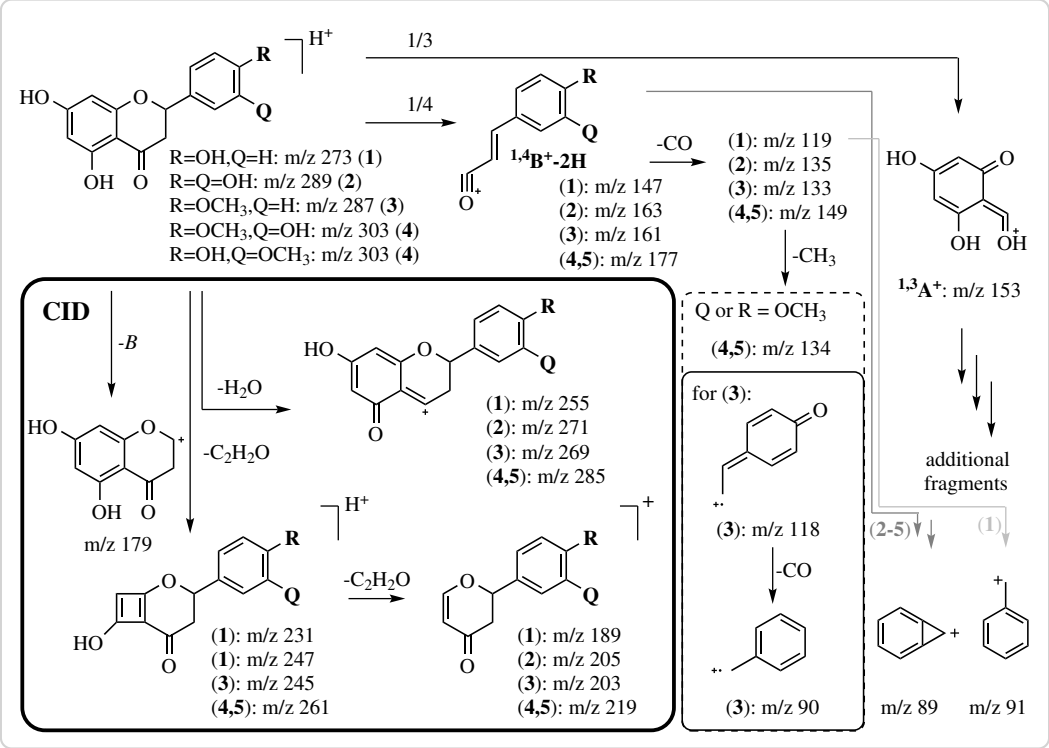

Figure 5.2.: *Major fragmentation pathways of flavanones. Activation using CID conditions at 45 % NCE mainly results in neutral losses of H_2O and ketene (C_2H_2O) from the molecular ion $[M+H]^+$ (bold frame). These neutral losses are scarcely observed when HCD with a NCE of 75 % or 100 % is used for activation. Here, C-ring cleavages followed by neutral losses from the cleavage fragments are dominant.*

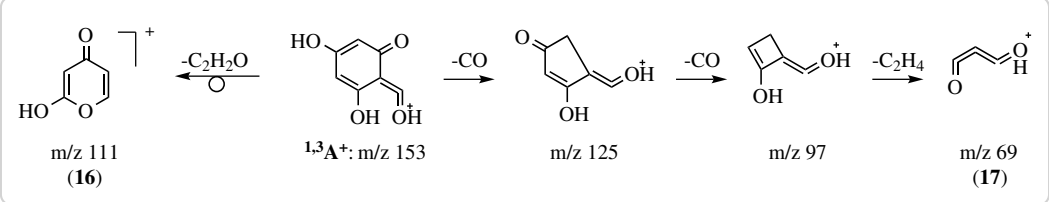

Figure 5.3.: *Proposed MS^2 fragmentation of $^{1,3}A^+$ after HCD activation. In high energy MS^2 experiments, $^{1,3}A^+$ might loose two CO followed by an unusual C_2H_4. A single loss of ketene (C_2H_2O) to afford m/z 111 is also sensible.*

at *m/z* 145. However, the loss of CO is the most prominent decomposition of ($^{1,4}B^+$-2H). The intensities of the peaks corresponding to the ($^{1,4}B^+$-2H-CO) fragment were as high as 36 % in HCD experiments (Figure 5.4). Naringenin (**1**) seems to

sequentially lose two CO in HCD mode to afford *m/z* 91 (intensities at 75 and 100 % NCE at 24 and 100 %, respectively). This *m/z* is a strong indicator of a benzylium or tropylium cation (Figure 5.2). Decay of ($^{1,4}B^+$-2H) of the other flavanones likely

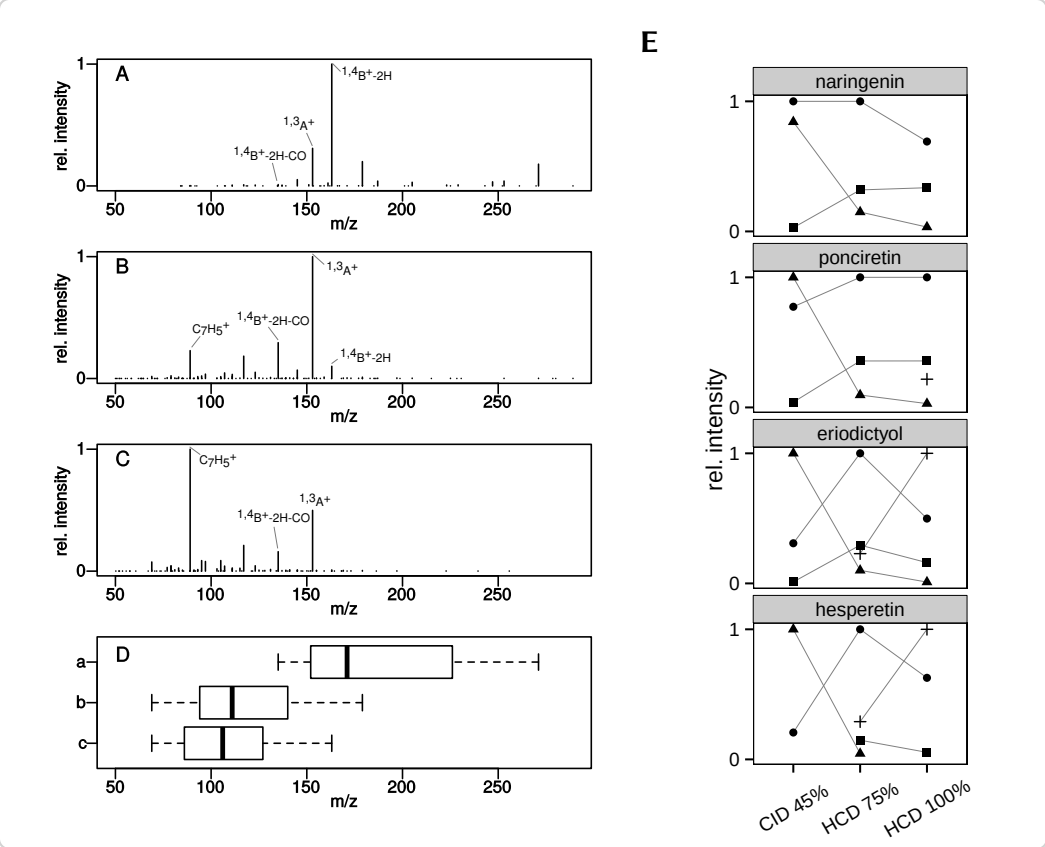

Figure 5.4.: *Comparison of CID and HCD MS^2 spectra of eriodictyol (**2**). **A** – CID at 45 % NCE. **B** – HCD at 75 % NCE. **C** – HCD at 100 % NCE. Four different prominent peaks are annotated in each spectrum. **D** – The shift to smaller masses in HCD spectra and with increasing NCE is illustrated by the boxplot of the distribution of peaks with relative intensities above 1 % in each of the above spectra. **E** – Relationship between the activation method and the intensity of four fragments (● $^{1,3}A^+$, ▲ ($^{1,4}B^+$-2H), ■ ($^{1,4}B^+$-2H-CO), + $C_7H_5^+$) of different flavanones.*

leads to a stable bicyclo[4.1.0]heptatrienyl cation as the high intensity of peak *m/z* 89 in HCD mode suggests. Methylated flavanones (**3**), (**4**) and (**5**) show a loss of CO followed by a loss of a methyl radical ($^{1,4}B^+$-2H-CO-CH3$^{\cdot}$), as suggested by the respective *m/z* values of 118 and 134. Another CO loss from this fragment is

possible for ponciretin (**3**) to produce an ion *m/z* 90, which is at 49 % intensity in the HCD spectrum recorded with NCE of 75 % . The evidence suggests, that this ion's structure is best described by a benzylium/tropylium radical cation (Figure 5.2). It is proposed, that ion $^{1,3}A^+$ can decompose via two different pathways under HCD conditions (Figure 5.3). A loss of ketene from $^{1,3}A^+$ results in *m/z* 111. Pyranone (**16**) is suggested as a structure for this ion. Sequential losses of two CO and a C_2H_4 could afford ion (**17**). However, further MS^n experiments are necessary to confirm these proposals.

5.3 Fragmentation of flavones

The principle fragmentation of flavone aglycones apigenin (**6**), luteolin (**7**), acacetin (**8**) and chrysoeriol (**10**) in positive mode CID tandem mass spectrometry was discussed previously [109, 129]. Non-methylated (**6**, **7**) and methylated flavones (**8** – **10**) show significantly different MS^2 spectra (Table B.12). Apigenín (**6**) and luteolin (**7**) MS^2 spectra show a characteristic *m/z* 153, corresponding to the $^{1,3}A^+$ ion, as a base peak in CID mode and at low activation energies in HCD mode (Figure 5.5). Contrary to the flavanones, the MS^2 of unmethylated flavones show the peak corresponding to the molecular ion $[M+H]^+$, which is strongest in HCD at NCE of 75 %. Characteristic neutral losses of water, CO and ketene (C_2H_2O) were also observed for (**6**) and (**7**) (Figure 5.5, Table B.12). MS-peaks corresponding to a loss of a formyl radical, resulting in $[M+H-CHO]^{\bullet+}$ were also observed for (**6**) and (**7**). Loss of ketene is proposed to proceed via two different pathways, such that further neutral losses of another ketene, or C_2H_2 might be explained (Figure 5.5). Besides the characteristic $^{1,3}A^+$ fragment, apigenin (**6**) and luteolin (**7**) MS^2 spectra also present peaks corresponding to the B-ring fragments $^{1,3}B^+$ (*m/z* 119 and 135) and $^{0,4}B^+$ (*m/z* 163 and 179). From the mass differences of these fragments, the substitution on the B-ring can be deduced. The $^{0,4}B^+$ ion might further degrade by neutral losses of ketene (32 Da) or water (18 Da). The base peaks at a NCE of 100 % in HCD, *m/z* 91 (**6**) and *m/z* 89 (**7**), are most likely due to a further decomposition of $^{1,3}B^+$ in a fashion similar to the flavanones to afford a benzylium or bicycloheptatrienyl cation respectively (Figure 5.5).

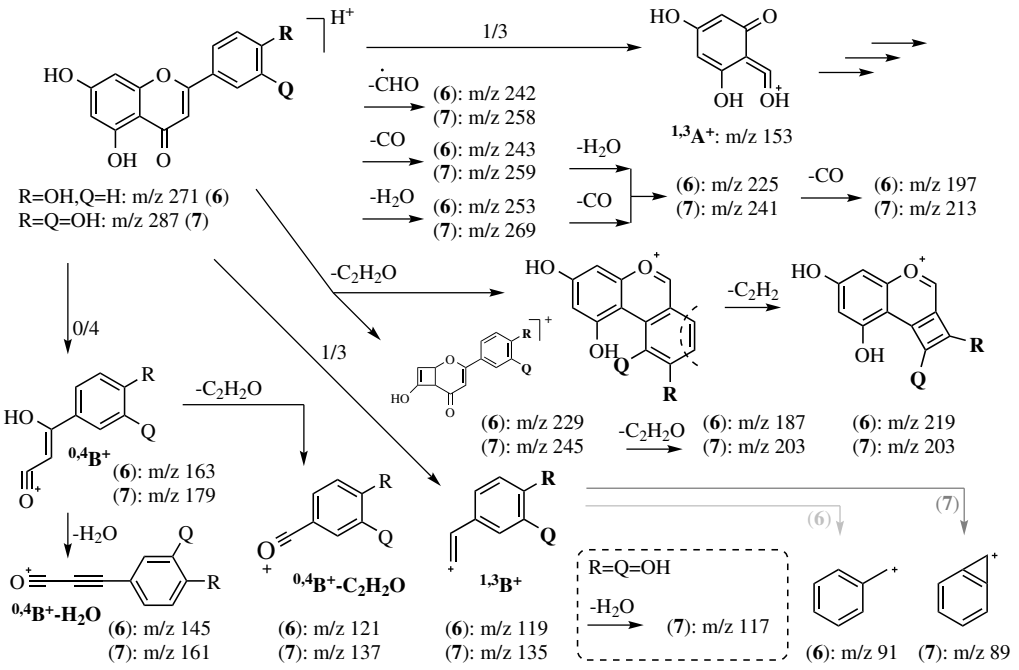

(a) Fragments characteristic for unmethylated flavones.

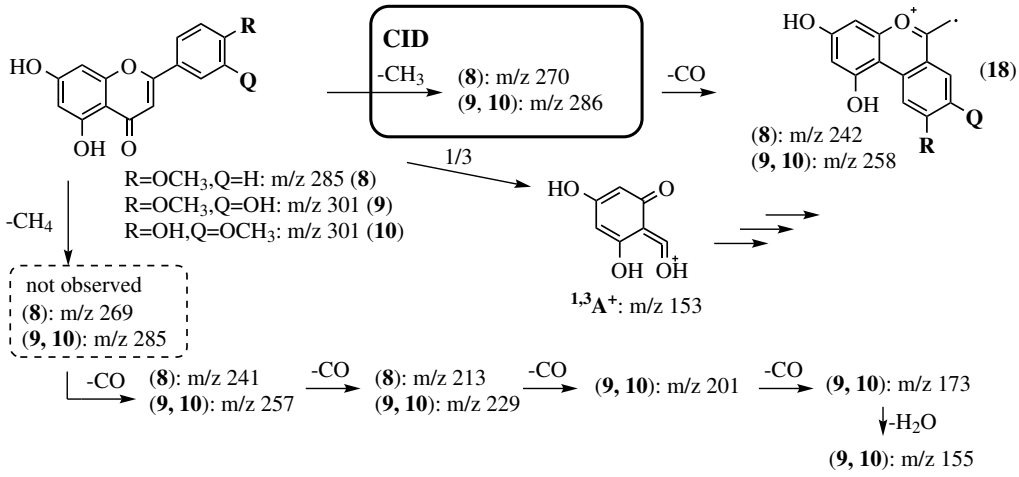

(b) Fragments characteristic for methylated flavones.

Figure 5.5.: *Major fragmentation pathways of unmethylated and methylated flavones. Multiple neutral losses of small molecules (e.g. CO, water or ketene) and 0/4 and 1/3 C ring cleavages are predominant in the MS^2 spectra of unmethylated flavones. Methylated flavones loose a methyl group in CID experiments, but only in HCD experiments do other fragmentation reaction become obvious.*

The most noteable difference between the methylated and unmethylated representatives is the almost complete lack of any fragmentation of the methylated flavones other than a methyl loss, in CID experiments (Table B.12, Figure 5.7). A relatively stable radical cation is formed after the loss of a methyl group, due to the fact that the whole system is essentially conjugated (Figure 5.6). Any other loss

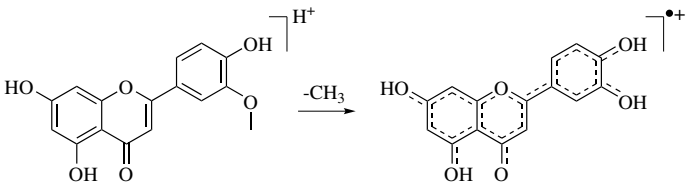

Figure 5.6.: *Stability of the $[M+H-CH_3]^{\bullet+}$ ion of flavones. The $[M+H-CH_3]^{\bullet+}$ ion of methylated flavones like diosmetin is highly stabilized by resonance, explaining the high intensity of the corresponding peak and limiting its fragmentation at low activation energies.*

would break this conjugation and therefore requires a higher activation energy. HCD experiments at NCE of (75 to 100) % were suitable to fragment the methylated flavones (**8**–**10**). The base peak in the HCD spectra of (**8**) (*m/z* 242) and (**9**, **10**) (*m/z* 257) at 75 % NCE was attributed to another loss of CO from the $[M+H-CH_3]^{\bullet+}$ ion, while the base peak *m/z* 153 at 100 % NCE likely corresponds to the $^{1,3}A^+$ ion (Figure 5.7). Further losses from $[M+H-CH_3-CO]^{\bullet+}$, with the proposed structure of a benzochromenylium radical (**20**), were not observed (Figure 5.5, Table B.12). Mass-to-charge ratios of 241 (**8**) and 257 (**9**, **10**) were attributed to a neutral loss of methane (CH_4), followed by a loss of CO (Figure 5.5, compound 5.8). Interestingly, the abundance of a peak corresponding to a $[M+H-CH_4]^+$ ion was below 1 % in all spectra, illustrating its susceptibility for additional losses. The fragment $[M+H-CH_4-CO]^+$ on the other hand might undergo further neutral losses of up to three CO (compounds **10** and **9**) as is illustrated for chrysoeriol in compound 5.8. However, instead of additional CO losses, fragment $[M+H-CH_3-2CO]^{\bullet+}$ of (**10**) or (**9**) might as well loose a C_2H_2 (compound 5.8), as suggested by the MS^2 spectra (Table B.12). The only C-ring fragmentation of the methylated flavones (**8**–**10**) occurs at positions 1/3, as the observed *m/z* 153 ($^{1,3}A^+$) suggests. The higher energy MS^2 spectra suggest, that the $^{1,3}A^+$ fragment might deteriorate further in the same manner as described for the flavanones (Figure 5.3). Numerous minor peaks in the MS^2 HCD

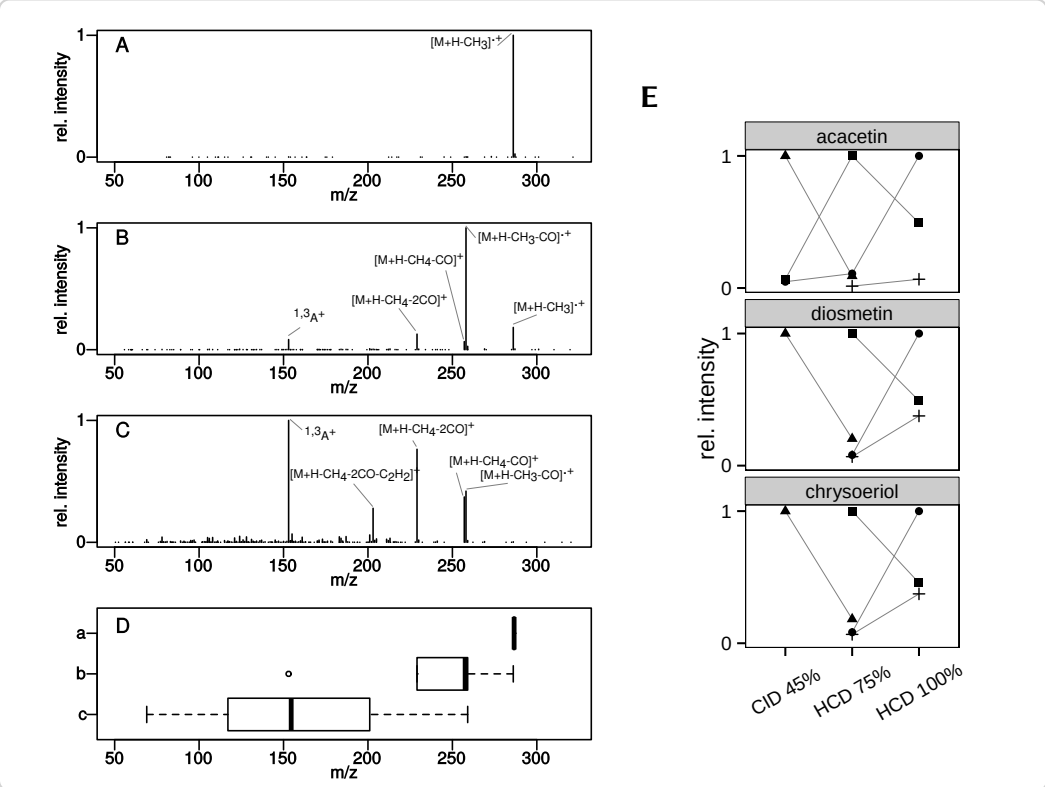

Figure 5.7.: *Comparison of CID and HCD MS^2 spectra of chrysoeriol (**10**). **A** – CID at 45 % NCE. **B** – HCD at 75 % NCE. **C** – HCD at 100 % NCE. Four different prominent peaks are annotated in each spectrum. **D** – The shift to smaller masses in HCD spectra and with increasing NCE is illustrated by the boxplot of the distribution of peaks with relative intensities above 1 % in each of the above spectra. **E** – Relationship between the activation method and the intensity of four fragments (● $^{1,3}A^+$, ▲ $[M+H\text{-}CH_3]^{\bullet+}$, ■ $[M+H\text{-}CH_3\text{-}CO]^{\bullet+}$, + $[M+H\text{-}CH_4\text{-}CO]^+$) of the studied methylated flavones.*

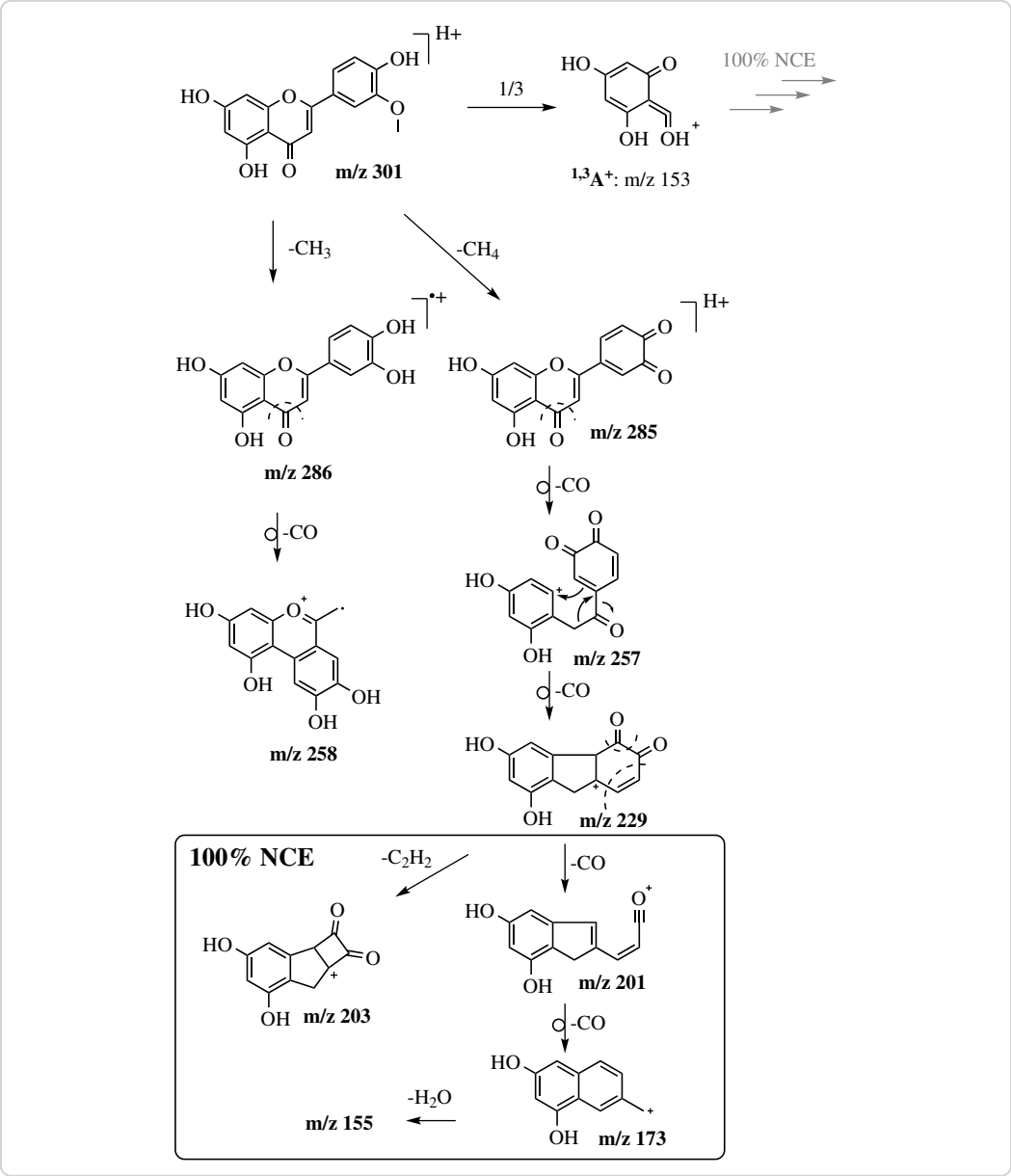

Figure 5.8.: *Proposed pathway of fragmentation of (**10**) after HCD activation. Losses of CH_3 textbullet and CH_4, followed by loss of CO are the major fragmentations observed in the corresponding MS spectra. However, multiple losses of CO only occur after a loss of methane (CH_4), possibly due to the relative stability of the benzochromenylium radical (**19**). At* 100 % *NCE even higher order fragmentations were observed.*

spectra of compounds (**8**–**10**) could not be assigned a fragment or structure, but many even numbered *m/z* values suggest quite complex rearrangements.

The general trend of smaller sized fragments at higher activation energies is also true for flavones (Figure 5.7).

5.4 Fragmentation of flavonols

The principle fragmentation pathways of kaempferol (**11**), quercetin (**12**), myricetin (**13**) and isorhamnetin (**15**) in CID tandem mass spectrometry have been previously reported [129, 134, 216]. Other than flavones, methylated and non-methylated flavonols share similar fragment(ation)s. Whereas in CID methylated flavons hardly showed any fragmentation beyond a methyl loss, methylated flavonoles kaempferide (**14**) and isorhamnetin (**15**) exhibited the same losses as their unmethylated couterparts, albeit at a much lower level (Table B.13, Figure 5.9 and 5.10). These observations are in full agreement with previous reports [129] and hold true in CID as well as HCD measurements. The observed losses from the molecular ion $[M+H]^+$ are essentially the same as those that were described for the flavones (**6**, **7**) (compare Figure 5.9 and 5.5). Lots of high intensity peaks presented in the MS^2 spectra of flavonoles and the base peaks changed between compounds. The base peak of (**11**) in the CID spectra was at *m/z* 165, which corresponds to the $^{0,2}A^+$ fragment (Figure 5.9). The signals *m/z* 257 and 273 corresponding to the $[M+H-H_2O]^+$ ions were the base peak in the CID-MS^2 spectra of (**12**) and (**13**) respectively. The $[M+H-CH_3]^{\bullet+}$ ions were highly abundant in the CID experiments of (**14**) and (**15**). The base peak of (**15**) *m/z* 302 corresponds to this fragment. Fragment ($^{0,3}A^+$ +2H) fits the *m/z* 139, which was the base peak in the CID spectrum of (**14**). The MS signal *m/z* 153 corresponding to fragment $^{1,3}A^+$ was at low abundance in CID spectra, especially for the methylated falvonols (Figure 5.10). However, in HCD experiments *m/z* 153 was the base peak of all flavonols, except kaempferide (**14**) where *m/z* 229 was at 100 % relative intensity.

Neutral losses of CO, water or a formyl radical are suggested by the collected spectra (Figure 5.9, Table B.13). Only for kaempferol (**11**), a neutral loss of 42 Da corresponding ketene was observed. However, MS^2 spectra of all flavonols, except

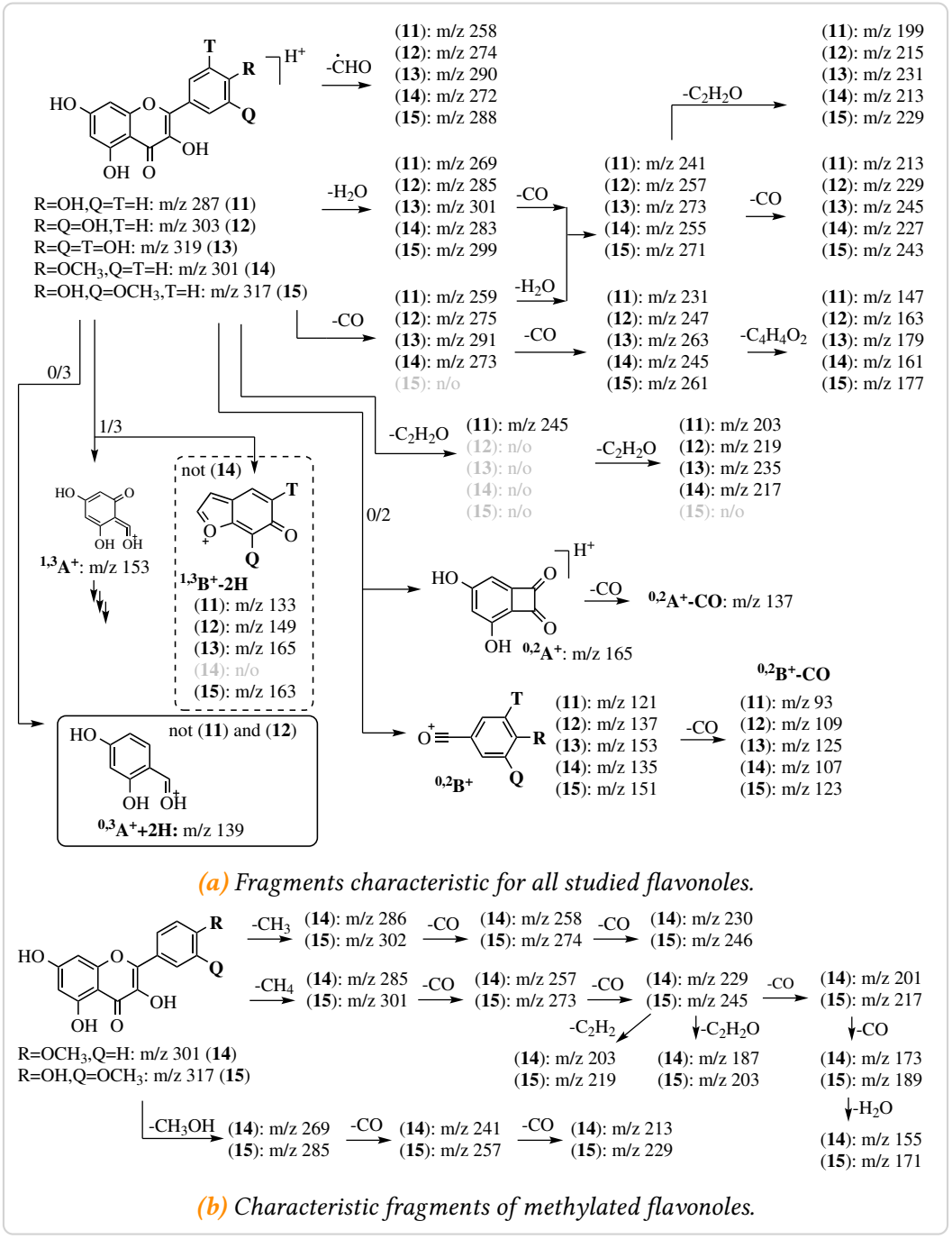

(a) Fragments characteristic for all studied flavonoles.

(b) Characteristic fragments of methylated flavonoles.

Figure 5.9.: *Major fragmentation pathways of flavonoles. Unlike flavones, methylated and unmethylated flavonoles share common fragmentations, albeit signals corresponding to small molecule losses are typically small for methylated analogues. Ring fragments observed typically correspond to the cleavage along bonds 0/3 or 0/2. Methylated flavonols shared common fragments with the methylated flavones.However, loss of methanol and a couple CO was also observed. n/o – not observed (relative intensity <1 %).*

(**15**), contained signals that could be assigned to the ion $[M+H-2C_2H_2O]^+$, suggesting a loss of two ketene units. This advocates the notion that the $[M+H-C_2H_2O]^+$ ion of flavonols might be highly unstable. Other than the flavones, flavonoles can loose two sequential CO and another $C_4H_4O_2$, confirming previously published data [129]. The spectra furthermore suggest, that the $[M+H-H_2O-CO]^+$ fragment of flavonols can loose another 42 Da (C_2H_2O), which was not spotted previously. The data also clearly show, that neutral losses off of the molecular ion are most abundant in CID experiments, whereas the shift to smaller masses in HCD experiments is obvious (Table B.13, Figure 5.10).

The studied flavonoles all displayed an MS signal at *m/z* 153 corresponding to the $^{1,3}A^+$ fragment, just as the flavanones and flavones with a 5,7-dihydroxy-substitution of the A-ring did. This further highlights the diagnostic nature of the $^{1,3}A^+$ fragment of flavonoids in MS/MS spectra. At higher energies, $^{1,3}A^+$ can further decompose in a manner discussed in the previous sections (Figure 5.3). Characteristic ring cleavage fragments of flavonols include $^{0,2}A^+$, $^{0,2}B^+$ and $^{1,3}B^+$-2H [129, 134], all of which were confirmed in the present study. Overall, the intensity of the $^{0,2}A^+$ and $^{1,3}B^+$-2H fragments decreased in HCD over CID experiments, whereas the intesity of ions $^{0,2}A^+$-CO, $^{0,2}B^+$ and $^{1,3}A^+$ increased (Figure 5.10).

Apart from the discussed fragmentations, MS^2 spectra of the methylated flavonols (**14**) and (**15**) also showed fragmentations typical of methyl esters, namely methyl, methane and methanol loss. Methyl and methane loss followed by sequential losses of carbon monoxide were already shown for flavones (**8**–**10**) and are postulated to proceed in a similar manner in flavonols (**14**) and (**15**) (Figure 5.11). Because of the extra hydroxyl at the C-ring, methylated flavonols such as isorhamnetin can loose two CO instead of just one after loss of a methyl radical (compare Figure 5.11 and (compound 5.8)). Other than flavones, spectra of methylated flavonols (**14**) and (**15**) also showed signals (*m/z* 269 and *m/z* 285) corresponding to a loss of methanol. The data suggests, that these $[M+H-CH_3OH]^+$ fragments can loose up to two CO, similar to the loss of water and CO (Figure 5.11 and 5.9). The peaks with *m/z* 301, 273, 245, 217 and 189 in the HCD spectra of isorhamnetin (**15**), suggest a loss of up to four CO after the inital loss of methane (Figure 5.11). As mentioned before, the smaller mass fragments corresponding to multiple neutral losses are more pronounced at

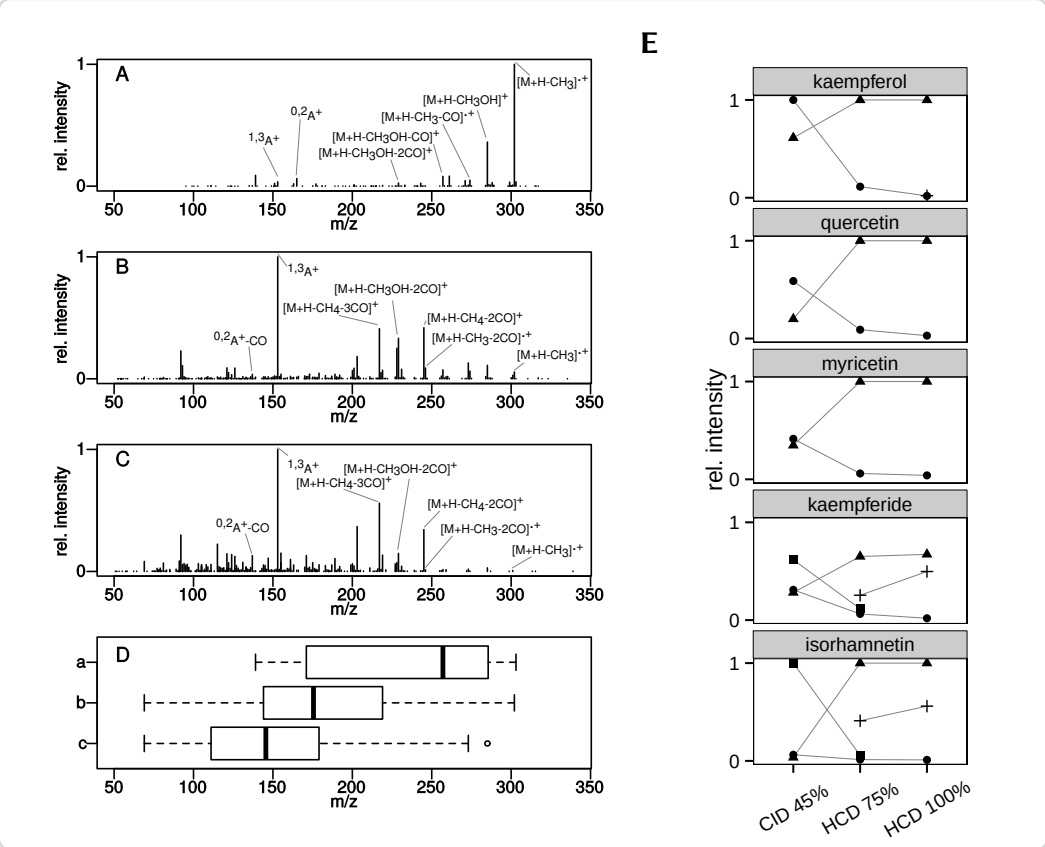

Figure 5.10.: *Comparison of CID and HCD MS^2 spectra of isorhamnetin (**15**). **A** – CID at 45 % NCE. **B** – HCD at 75 % NCE. **C** – HCD at 100 % NCE. Four different prominent peaks are annotated in each spectrum. **D** – The shift to smaller masses in HCD spectra and with increasing NCE is illustrated by the boxplot of the distribution of peaks with relative intensities above 1 % in each of the above spectra. **E** – Relationship between the activation method and the intensity of four fragments (● $^{0,2}A^+$, ▲ $^{1,3}A^+$, ■ $[M+H\text{-}CH_3]^{\bullet+}$, + $[M+H\text{-}CH_4\text{-}3CO]^+$) of the studied methylated flavones.*

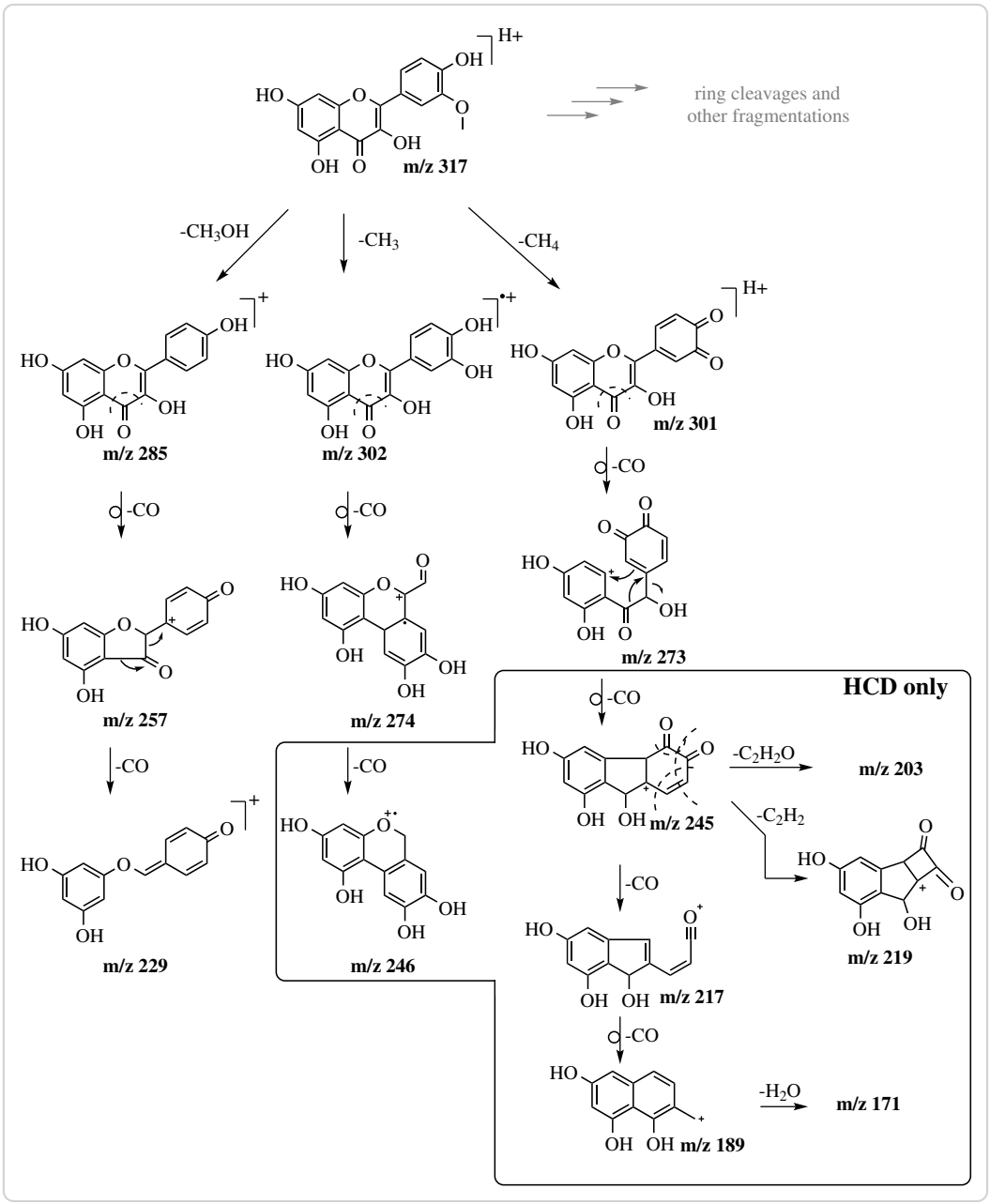

*Figure 5.11.: Proposed pathways of fragmentation of isorhamnetin (**15**). Isorhamnetin might loose methyl, methane or methanol upon activation. A similar fragmnentation pathway was proposed for the analogous chrysoeriol (compound 5.8). Some fragmentations were observed in HCD mode only (box).*

higher activation energies and were thus limited to HCD experiments at a NCE of 100 % (Figure 5.10, Figure 5.11).

5.5 Conclusions and Discussion

This comprehensive study shows that, taken together, data from CID and HCD experiments can be complementary to give a much deeper understanding of structural features of flavonoids. Mass errors were calculated for each postulated fragment and ranged from (0.4 to 10) ppm, highlighting the accuracy of the instrument which also allowed for the accurate determination of molecular formulas from MS signals.

The complementary nature of CID and HCD is especially stricking, when comparing spectra of (**9**) and (**10**). CID fragmentation of these B-ring methylated flavones afforded MS spectra, where a methyl loss was by far the dominant fragmentation. HCD on the other hand provided higher order fragmentations combined with a higher signal-to-noise ratio, for a deeper insight into structural features. These higher order fragmentations were accelerated by increasing the activation energy, but interpretability of the corresponding spectra was limited. However, with the help of *in silico* methods for the interpretation of MS/MS spectra [14, 215] and the computing power available today, the information contained in highly complex spectra might become more easily accecible. Nonetheless, fine-tuning of the activation energy is an option to optimize fragmentation intensities, especially of the C-ring fragmentations.

Flavones and flavonols share similar patterns of fragmentation and display a loss of a CHO radical, which distinguishes their MS^2 spectra from those of the flavanones. Distinguishing characteristics between MS^2 spectra of flavones and flavonols are the C-ring fragmentations, where the $^{0,4}B^+$ fragment was typically limited to flavones, whereas a (strong) $^{0,2}A^+$ fragment was only observed for (unmethylated) flavonols. While methylated flavanones did not differ in their fragmentations from their non-methylated analogues, MS spectra of methylated and non-methylated flavones and flavonols showed significant differences. Noticable loss of $CH_3^{\bullet}$ or CH_4, followed by losses of CO were typical signs of methylated flavones or flavonols. Loss of methanol was observed in methylated flavonols and

in small amounts at 100 % NCE in flavones, not however in the MS^2 spectra of flavanones. Under the right conditions, all of the studied 5,7-dihydroxy substituted flavonoids presented a $^{1,3}A^+$ ion, with a characteristic *m/z* 153. This information might be of value for studies that want to determine the position of a derivatization of the flavonoid core. To the authors knowledge, a pathway for the decomposition of $^{1,3}A^+$ at high activation energies was proposed for the first time in this work and is universal for all studied compounds. A signal *m/z* 91, stemming from the decay of the $^{1,4}B^+$ or $^{1,3}B^+$ ion, might be a hint for a *para*-monohydroxylated B-ring on flavanones and flavones respectively. Conversely, a peak *m/z* 89 can point in the direction of multiple substitutions on the B-ring.

In summary, the complementary nature of the studied activation methods CID and HCD provides more thourough data for the study of flavonoids. Key ions might only present themselves in the spectra of either method, and together with differences and similarities in the MS/MS spectra, can be used to gain additional insights into the structural characteristics of a studied compound.

5.6 Contributions

Benjamin Weigel prepared substances, analyzed mass spectral data and prepared manuscript. Annegret Laub and Jürgen Schmidt conducted LC/MS measurement runs. Through helpful discussions, Jürgen Schmidt helped tremendously with the preparation of the manuscript.

Table B.11.: *Key ions in the positive mode CID and HCD ESI-MS^2 spectra of flavanones.*

	fragment	**CID,** 45 % **NCE**					**HCD,** 75 % **NCE**					**HCD,** 100 % **NCE**				
		(1)	**(2)**	**(3)**	**(4)**	**(5)**	**(1)**	**(2)**	**(3)**	**(4)**	**(5)**	**(1)**	**(2)**	**(3)**	**(4)**	**(5)**
2	$[M+H-H_2O]^+$	255 (1)	271 (18)	269 (1)	285 (10)	285 (4)										
4	$[M+H-C_2H_2O]^+$	231 (4)	247 (3)	245 (3)	261 (2)	261 (2)										
5	$[M+H-2C_2H_2O]^+$	189 (5)	205 (3)	203 (4)	219 (2)	219 (1)										
8	AC^+	179 (4)	179 (20)	179 (5)	179 (28)	179 (30)		179 (1)		179 (2)	179 (2)				179 (2)	179 (1)
11	$1,3A^+$	153 (100)	153 (31)	153 (77)	153 (21)	153 (57)	153 (100)	153 (100)	153 (100)	153 (100)	153 (100)	153 (69)	153 (50)	153 (100)	153 (63)	153 (58)
12	$1,3A^+-CO$											125 (1)		125 (1)	125 (1)	
13	$1,3A^+-C_2H_2O$							111 (2)	111 (1)	111 (1)		111 (2)	111 (2)	111 (4)	111 (2)	111 (2)
14	$1,3A^+-2CO$						97 (3)	97 (4)	97 (3)	97 (4)	97 (4)	97 (10)	97 (8)	97 (15)	97 (9)	97 (9)
15	$1,3A^+-2CO-C_2H_4$						69 (2)	69 (2)	69 (2)	69 (2)	69 (2)	69 (9)	69 (8)	69 (13)	69 (9)	69 (8)
17	$1,4B^+-2H$	147 (84)	163 (100)	161 (100)	177 (100)	177 (100)	147 (15)	163 (10)	161 (10)	177 (4)	177 (2)	147 (3)	163 (1)	161 (3)		
18	$1,4B^+-2H-H_2O$		145 (5)					145 (7)					145 (1)			
19	$1,4B^+-2H-CO$	119 (3)	135 (1)	133 (4)			119 (32)	135 (29)	133 (36)	149 (15)	149 (11)	119 (34)	135 (16)	133 (36)	149 (5)	149 (3)
20	$1,4B^+-2H-CO-CH_3$								118 (11)	134 (11)	134 (7)			118 (57)	134 (20)	134 (13)
22	$1,4B^+-2H-2CO$						91 (24)					91 (100)				
23	$1,4B^+-2H-2CO-CH_3$								90 (3)					90 (49)		
24	$1,4B^+-2H-C_2H_2O-H_2O$									117 (15)	117 (32)				117 (13)	117 (26)
25	$1,4B^+-2H-H_2O-CO$							117 (18)					117 (21)			
26	$C_7H_7^+$						91 (24)		91 (1)	91 (3)	91 (2)	91 (100)		91 (5)	91 (7)	91 (5)
27	$C_7H_5^+$							89 (23)		89 (29)	89 (24)		89 (100)	89 (22)	89 (100)	89 (100)

Table B.12.: *Key ions in the positive mode CID and HCD ESI-MS^2 spectra of flavones.*

	fragment	**CID**, 45 % **NCE**					**HCD**, 75 % **NCE**					**HCD**, 100 % **NCE**				
		(**6**)	(**7**)	(**8**)	(**9**)	(**10**)	(**6**)	(**7**)	(**8**)	(**9**)	(**10**)	(**6**)	(**6**)	(**7**)	(**9**)	(**10**)
1	$[M+H]^+$	271 (2)					271 (84)	287 (66)	285 (4)			271 (2)	287 (2)			
2	$[M+H-CH_3]^{\bullet+}$			270 (100)	286 (100)	286 (100)			270 (9)	286 (20)	286 (18)					
3	$[M+H-H_2O]^+$	253 (1)	269 (9)				253 (3)	269 (6)								
4	$[M+H-CO]^+$	243 (7)	259 (9)				243 (7)					243 (2)				
5	$[M+H-CHO]^{\bullet+}$	242 (14)	258 (47)				242 (1)	258 (3)				242 (2)	258 (2)			
6	$[M+H-C_2H_2O]^+$	229 (21)	245 (13)	243 (1)			229 (4)									
7	$[M+H-CH_3-CO]^{\bullet+}$			242 (7)					242 (100)	258 (100)	258 (100)			242 (49)	258 (49)	258 (46)
8	$[M+H-CH_4-CO]^+$								241 (1)	257 (7)	257 (7)			241 (7)	257 (38)	257 (37)
9	$[M+H-H_2O-CO]^+$	225 (13)	241 (13)				225 (4)	241 (16)					241 (4)			
14	$[M+H-CH_4-2CO]^+$									229 (12)	229 (13)			213 (6)	229 (75)	229 (76)
15	$[M+H-H_2O-2CO]^+$		213 (2)				197 (4)	213 (7)				197 (3)	213 (4)			
16	$[M+H-2C_2H_2O]^+$	187 (3)	203 (4)				187 (2)	203 (2)				187 (1)	203 (3)			
17	$[M+H-CH_3OH-2CO]^{\bullet+}$							199 (1)							213 (4)	213 (4)
18	$[M+H-CH_4-2CO-C_2H_2]^+$														203 (29)	203 (31)
20	$[M+H-CH_4-3CO]^+$												187 (2)	185 (1)	201 (7)	201 (6)
23	$[M+H-CH_4-4CO]^+$											143 (1)			173 (3)	173 (2)
24	$[M+H-2CO-2C_2H_2O]^+$						131 (2)	147 (1)				131 (5)	147 (3)		161 (4)	161 (5)
27	$0,4B^+$	163 (6)	179 (7)				163 (8)	179 (3)				163 (2)				
28	$0,4B^+-H_2O$	145 (13)	161 (12)				145 (17)	161 (16)				145 (41)	161 (29)			
25	$0,4B^+-C_2H_2O$	121 (6)	137 (7)				121 (16)	137 (12)				121 (25)	137 (16)			
29	$1,3A^+$	153 (100)	153 (100)	153 (5)			153 (100)	153 (100)	153 (11)	153 (8)	153 (8)	153 (84)	153 (87)	153 (100)	153 (100)	153 (100)
30	$1,3A^+-CO$						125 (1)	125 (2)				125 (3)	125 (2)			
31	$1,3A^+-C_2H_2O$						111 (2)	111 (2)				111 (4)	111 (3)		111 (1)	111 (1)
32	$1,3A^+-2CO$						97 (2)	97 (2)				97 (9)	97 (9)	97 (1)	97 (2)	97 (2)
33	$1,3A^+-2CO-C_2H_4$						69 (4)	69 (5)				69 (24)	69 (22)	69 (1)	69 (2)	69 (2)
34	$1,3B^+$	119 (12)	135 (11)	133 (2)			119 (49)	135 (40)	133 (3)			119 (35)				
35	$1,4A^++2H$							127 (1)					127 (2)			
39	$C_7H_7^+$	91 (1)					91 (26)					91 (100)				
40	$C_7H_5^+$							89 (17)				89 (7)	89 (100)	89 (3)		89 (1)

Table B.13.: *Key ions in the positive mode CID and HCD ESI-MS^2 spectra of flavonoles.*

	fragment	CID, 45 % NCE					HCD, 75 % NCE					HCD, 100 % NCE				
		(11)	(12)	(13)	(14)	(15)	(11)	(12)	(13)	(14)	(15)	(11)	(12)	(13)	(14)	(15)
1	$[M+H]^+$						287 (25)	303 (8)	319 (1)	301 (9)						
2	$[M+H-CH_3]^{\bullet+}$				286 (62)	302 (100)				286 (12)	302 (6)					
3	$[M+H-CH_4]^+$				285 (2)					285 (5)	301 (3)				285 (1)	
4	$[M+H-H_2O]^+$	269 (32)	285 (63)	301 (40)	283 (2)	299 (3)	269 (2)	285 (6)	301 (1)			269 (2)	285 (3)			
5	$[M+H-CO]^+$	259 (24)	275 (14)	291 (6)	273 (3)		259 (3)									
6	$[M+H-CHO]^{\bullet+}$	258 (46)	274 (20)	290 (22)	272 (20)	288 (3)	258 (10)	274 (4)		272 (2)						
7	$[M+H-CH_3OH]^{\bullet+}$				269 (11)	285 (36)				269 (11)	285 (11)				269 (3)	285 (3)
9	$[M+H-C_2H_2O]^+$	245 (4)														
10	$[M+H-CH_3-CO]^{\bullet+}$				258 (9)	274 (5)				258 (58)	274 (6)				258 (2)	
12	$[M+H-CH_4-CO]^+$				257 (3)					257 (17)	273 (13)				257 (6)	273 (2)
13	$[M+H-H_2O-CO]^+$	241 (99)	257 (100)	273 (100)	255 (3)	271 (5)	241 (5)	257 (13)	273 (6)			241 (1)	257 (2)			
14	$[M+H-2CO]^+$	231 (40)	247 (37)	263 (25)	245 (17)	261 (8)	231 (5)	247 (2)								
15	$[M+H-CH_3OH-CO]^{\bullet+}$				241 (16)	257 (8)				241 (2)	257 (7)					257 (2)
17	$[M+H-CH_3-2CO]^{\bullet+}$						216 (2)	232 (2)		230 (94)	246 (9)	216 (2)			230 (9)	
19	$[M+H-CH_4-2CO]^+$									229 (100)	245 (42)				229 (100)	245 (34)
20	$[M+H-H_2O-2CO]^+$	213 (77)	229 (70)	245 (32)	227 (2)	243 (2)	213 (20)	229 (49)	245 (22)	227 (2)		213 (12)	229 (16)	245 (6)		
21	$[M+H-3CO]^+$						203 (2)		235 (2)							
22	$[M+H-2C_2H_2O]^+$	203 (7)	219 (4)	235 (4)	217 (2)			219 (1)				203 (1)	219 (2)			
23	$[M+H-H_2O-CO-C_2H_2O]^{\bullet+}$	199 (3)	215 (2)	231 (2)	213 (4)	229 (3)			231 (1)	213 (11)	229 (33)				213 (10)	229 (15)
23	$[M+H-CH_3OH-2CO]^{\bullet+}$				213 (4)	229 (3)				213 (11)	229 (33)				213 (10)	229 (15)
24	$[M+H-CH_4-2CO-2C_2H_2]^+$									203 (3)	219 (7)				203 (11)	219 (13)
25	$[M+H-H_2O-2CO-C_2H_2]^+$							203 (3)	219 (8)	201 (25)	217 (41)	187 (2)	203 (10)	219 (21)	201 (50)	217 (56)
26	$[M+H-CH_4-3CO]^+$									201 (25)	217 (41)				201 (50)	217 (56)
27	$[M+H-CH_4-2CO-C_2H_2O]^+$									187 (4)	203 (18)				187 (13)	203 (37)
28	$[M+H-CH_4-4CO]^+$									173 (2)	189 (4)				173 (13)	189 (11)
29	$[M+H-2CO-2C_2H_2O]^+$	147 (13)	163 (7)	179 (7)	161 (13)	177 (2)	147 (9)	163 (7)	179 (9)	161 (4)		147 (8)	163 (5)	179 (9)		
31	$0,2A^+$	165 (100)	165 (59)	165 (41)	165 (31)	165 (6)	165 (11)	165 (9)	165 (6)	165 (6)	165 (1)	165 (2)	165 (3)	165 (4)	165 (2)	165 (1)
32	$0,2A^+-CO$	137 (11)	137 (23)	137 (6)	137 (4)		137 (14)	137 (47)	137 (15)	137 (7)	137 (4)	137 (12)	137 (38)	137 (32)	137 (8)	137 (13)
33	$0,2B^+$	121 (36)	137 (23)	153 (35)	135 (18)	151 (2)		137 (47)	153 (100)	135 (14)	151 (2)	121 (69)	137 (38)	153 (100)	135 (5)	151 (1)
35	$0,3A^++2H$				139 (100)	139 (9)			139 (3)	139 (7)	139 (1)			139 (3)	139 (4)	
37	$1,3A^+$	153 (61)	153 (20)	153 (35)	153 (28)	153 (4)		153 (100)	153 (100)	153 (65)	153 (100)	153 (100)	153 (100)	153 (100)	153 (67)	153 (100)
38	$1,3A^+-CO$								125 (3)			125 (2)	125 (1)	125 (5)		
39	$1,3A^+-C_2H_2O$	111 (19)	111 (7)	111 (4)			111 (5)	111 (6)	111 (6)	111 (1)		111 (4)	111 (5)	111 (7)	111 (3)	111 (6)
40	$1,3A^+-2CO$						97 (2)	97 (2)	97 (3)			97 (9)	97 (10)	97 (14)	97 (3)	97 (3)
41	$1,3A^+-2CO-C_2H_4$						69 (7)	69 (8)	69 (8)	69 (3)	69 (1)	69 (33)	69 (31)	69 (29)	69 (10)	69 (8)
42	$1,3B^+-2H$	133 (25)	149 (10)	165 (41)		163 (2)	133 (3)	149 (3)	165 (6)		163 (1)	133 (1)	149 (4)	165 (4)	147 (3)	163 (5)
49	$C_7H_7^+$						91 (2)	91 (2)	91 (2)	91 (4)						
50	$C_7H_5^+$											89 (6)	89 (9)	89 (7)	89 (2)	89 (2)